Multiple Marine Vehicle Deconflicted Path Planning with Currents and Communication Constraints ⋆

Andreas J. Häusler * **Reza Ghabcheloo** **
António M. Pascoal * **A. Pedro Aguiar** *

* *Institute for Systems and Robotics, Dept. of Electrical Engineering, Instituto Superior Técnico, Av. Rovisco Pais No. 1, 1049-001 Lisboa, Portugal. (e-mail: {ahaeusler,antonio,pedro}@isr.ist.utl.pt)*
** *Department of Intelligent Hydraulics and Automation, Tampere Univ. of Technology, P.O. Box 589, 33101 Tampere, Finland. (e-mail: reza.ghabcheloo@tut.fi)*

Abstract: Recent research in multiple autonomous marine vehicle (AMV) applications shows that versatile path planning algorithms are of crucial importance to cooperative control scenarios. These algorithms need to be lightweight in terms of running time and capable of incorporating different factors influencing a given mission, like AMV dynamic constraints and environmental conditions. In addition, the path planner needs to take into account requirements imposed by multiple vehicle scenarios (of which collision avoidance is an important issue), and inter-vehicle communication constraints. Mission-related measures have to be incorporated additionally, such as minimization of energy usage over all participating AMVs, and simultaneous arrival of the AMVs at their designated target destinations, to name but a few. These aspects pose considerable challenges both from a theoretical and practical implementation standpoint.
This paper presents a versatile path planning algorithm for deconflicted multiple AMV missions at sea, incorporating single vehicle dynamical constraints as well as an inter-vehicle communication constraint. Additionally, it takes into account unknown constant ocean currents, and gives an overview on time-coordinated path following, a a closed-loop methodology to execute the planned mission, reducing the need for replanning in the presence of disturbances. The paper finishes with an outlook on important future directions to advance the algorithm.

Keywords: Deconflicted Path Planning, Multiple Autonomous Marine Vehicles, Time-Coordinated Path Following.

1. INTRODUCTION

As versatility and usability of autonomous robots increases, more and more new frontiers are available to be explored by robots in all kinds of environments. Land, air, space and marine robots pose active areas of research, boosting exciting developments continuously. This development is also reflected in marine robotics, as ever increasing sophistication leads to a growing range of possible applications, amongst whose the most appealing are those with the capability of reducing danger for humans in dangerous environments.

The marine environment poses a rich field of challenges to multiple vehicle control systems to be dealt with, such as sea waves, ocean currents, low underwater visibility, lack of global positioning data under water, and stringent acoustic communication constraints. Central to the implementation of systems that are able to cope with all named conditions is the availability of a multiple vehicle path planning algorithm, which can take into account the constraints of each vehicle as well as important environmental conditions.

Figure 1 illustrates the problem at hand and shows how a cost criterion, initial and final vehicle conditions, and internal and external constraints are used to produce (if it exists) a trajectory that meets the constraints and minimizes the cost. The spatial and temporal coordinates of this trajectory yield a spatial path and a corresponding velocity profile.

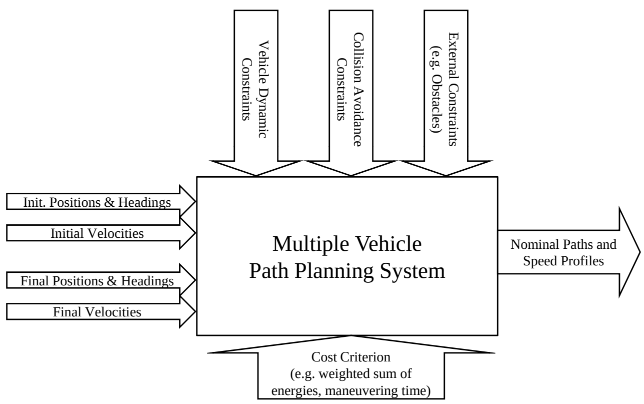

Fig. 1. Schema of the path planning system.

⋆ Research supported in part by the $FREE_{\text{sub}}NET$ Research Training Network of the EU FP6 under contract number MRTN-CT-2006-036186 (http://www.freesubnet.eu), project NAV-Control/FCT-PT (PTDC/EEA-ACR/65996/2006) of the CMU-Portugal program, project Co^3-AUVs of the EU FP7 under grant agreement number 231378 (http://www.Co3-AUVs.eu), the FCT-ISR/IST plurianual funding, and the Academy of Finland.

This problem and the solutions we propose have been strongly influenced by several mission scenarios studied in the scope of the two EU research projects described in $FREE_{\text{sub}}NET$ (2006–2010) and GREX (2006–2009). Previous work on deconflicted path planning for multiple marine vehicles was recently published in Häusler et al. (2009a,b). In this paper, we propose advancements of the algorithm in terms of versatility as well as from the optimization point of view, and we point out future improvements which we plan to pursue.

The path planning technique on which we rely is based on work of Kaminer et al. (2006) for unmanned air vehicles. The key idea, originally reported by Yakimenko (2000), is to separate spatial and temporal path specifications, which allows for decoupling the process of spatial path computation from that of computing the desired speed profiles for the vehicles along the paths. This decoupling is achieved by parameterizing each path as a set of polynomials in terms of a generic variable τ and introducing a polynomial function $\eta(\tau)$, that specifies the rate of evolution of τ with time, that is, $d\tau/dt = \eta(\tau)$, see Kaminer et al. (2007). By restricting the polynomials to be of low degree, the number of parameters used during the computation of the optimal paths is kept to a minimum. Once the order of the polynomial parameterizations has been decided, we can solve the given multiple vehicle path planning problem by applying e.g. the zero-order optimization technique described in Hooke and Jeeves (1961), from now on referred to as "H&J".

Our paper is organized as follows. In Sec. 2 we give a short description of the theory behind the means of path generation we employ. Sec. 3 introduces the multiple vehicle path planning problem and shortly discusses the concept of spatially versus temporally deconflicted paths, as well as the optimization approach for multiple vehicles. Currents and communication constraints are added to the algorithm in form of environmental constraints in Sec. 4, where we also show simulation results. In Sec. 5, we put Sec. 6 shows the connection of the generated paths and velocity profiles to a path following controller, while Sec. 7 gives a final outlook on upcoming changes of our algorithm.

2. POLYNOMIAL PATH PLANNING

In this section, we give a short introduction to our approach to path generation for the single vehicle case. Due to space limitations, some important details have to be omitted. The complete theoretical framework is being dealt with in all its extent in Häusler et al. (2009a).

2.1 Path polynomials.

Let us begin by recalling the difference between paths and trajectories. A path is a curve $\bar{p} : \tau \to \mathbb{R}^3$, parameterized by τ in a closed subset $[0, \tau_f]$ with $\tau_f > 0$. If τ is identified with time t or a function of time, then (remark the notation without bar), $p : t \to \mathbb{R}^3$ with $t \in [0, t_f], t_f > 0$ will be called a trajectory. *Path following* refers to the problem of making a vehicle converge to and following a path $\bar{p}(\tau)$ with no explicit temporal schedule. However, the vehicle speed may be assigned as a function of parameter τ. *Trajectory tracking* is the problem of making the vehicle track a trajectory $p(t) = \bar{p}(\tau(t))$, that is, the vehicle must satisfy spatial and temporal schedules simultaneously. The difference is that trajectory tracking depends on absolute timing, which does not allow for on-line modification of the plan in case of disturbances during execution. On the other hand, in the case path following, if the vehicle for any reason cannot follow the desired speed or stops for some time, it still can continue following the path with the given speed profile. See Häusler et al. (2009b) for more detail.

The key point of our technique, as first introduced by Yakimenko (2000) and later on extended by Kaminer et al. (2006, 2007), is the separation of spatial and temporal path description. (For a thorough supportive argumentation, please refer to Häusler et al. (2009b).) Due to this separation, the optimization process can be viewed as a method to produce paths $\bar{p}_i(\tau_i)$ without explicit time constraints, but with timing laws $\eta_i(\tau)$ that effectively dictate how the nominal speed of each vehicle should evolve along the path. Using this set-up, spatial and temporal constraints are essentially decoupled and captured in the descriptions of $\bar{p}_i(\tau_i)$ and $\eta_i(\tau) = d\tau_i/dt$, respectively, as will be seen later. Furthermore, adopting polynomial approximations for $\bar{p}_i(\tau_i)$ and $\eta_i(\tau)$ keeps the number of optimization parameters small and makes real-time computational requirements easy to achieve. Intuitively, by making the path of a generic vehicle V_i a polynomial function of $\tau_i \in [0, \tau_{f_i}]$, the shape of the path in space can be changed by increasing or decreasing τ_{f_i}—a single optimization parameter. This, coupled with a polynomial approximation for $\eta_i(\tau_i)$ makes it easy to shape the speed and acceleration profile of the vehicle along the path so as to meet desired dynamical constraints.

Consider now the path of a single vehicle, denoted by $\bar{p}(\tau) = [\bar{x}(\tau), \bar{y}(\tau), \bar{z}(\tau)]^\top$ with a parameterization $\tau = [0, \tau_f]$. Each coordinate $\bar{x}(\tau)$, $\bar{y}(\tau)$ and $\bar{z}(\tau)$ can be represented by an algebraic polynomial of degree N, i.e. $\bar{x}(\tau) = \sum_{k=0}^{N} a_{xk}\tau^k$. The minimum degree $N^\star$ of each polynomial is specified by the number of boundary conditions to be met; see Häusler et al. (2009a). If desired, additional degrees of freedom can be included by making $N > N^\star$. For the remainder of the paper, we use $N = 5$, which gives us the equation

$$\begin{pmatrix} 1 & 0 & 0 & 0 & 0 & 0 \\ 0 & 1 & 0 & 0 & 0 & 0 \\ 0 & 0 & 2 & 0 & 0 & 0 \\ 1 & \tau_f & \tau_f^2 & \tau_f^3 & \tau_f^4 & \tau_f^5 \\ 0 & 1 & 2\tau_f & 3\tau_f^2 & 4\tau_f^3 & 5\tau_f^4 \\ 0 & 0 & 2 & 6\tau_f & 12\tau_f^2 & 20\tau_f^3 \end{pmatrix} \cdot \begin{pmatrix} a_{x,0} \\ a_{x,1} \\ a_{x,2} \\ a_{x,3} \\ a_{x,4} \\ a_{x,5} \end{pmatrix} = \begin{pmatrix} \bar{x}(0) \\ \bar{x}'(0) \\ \bar{x}''(0) \\ \bar{x}(\tau_f) \\ \bar{x}'(\tau_f) \\ \bar{x}''(\tau_f) \end{pmatrix} \quad (1)$$

to compute the coefficients of $\bar{x}(\tau)$. $\bar{x}'$ and $\bar{x}''$ denote first and second "spatial" derivatives of $\bar{x}$ towards τ. Given $\eta(\tau)$, the (spatial) boundary conditions on the right-hand side of (1) can be computed from given (temporal) boundaries using formulas described in Häusler et al. (2009b,a); Ghabcheloo et al. (2009).

To shape the speed profile along a trajectory $p(t)$, we now need to define means of including temporal constraints in the computation process for a feasible path. This can be achieved by choosing $\eta(\tau) = d\tau/dt$, which describes the evolution of τ in time, giving us equations for temporal speed $v(\tau(t))$ and acceleration $a(\tau(t))$ (we write τ for $\tau(t)$)

$$\begin{aligned} v(\tau) &= \eta(\tau)\sqrt{\bar{x}'^2(\tau) + \bar{y}'^2(\tau) + \bar{z}'^2(\tau)} = \eta(\tau)||\bar{p}'(\tau)|| \\ a(\tau) &= ||\bar{p}''(\tau)\eta^2(\tau) + \bar{p}'(\tau)\eta'(\tau)\eta(\tau)|| \end{aligned} \quad (2)$$

Choosing a particular $\eta(\tau)$, it follows from (2) that a path $\bar{p}(\tau)$ is feasible if all boundary conditions are met, together with additional speed and acceleration constraints that can now be specified as

$$\begin{aligned} &v_{\min} \le \eta(\tau)||\bar{p}'(\tau)|| \le v_{\max}, \\ &||\bar{p}''(\tau)\eta^2(\tau) + \bar{p}'(\tau)\eta'(\tau)\eta(\tau)|| \le a_{\max} \ \forall \tau \in [0, \tau_f]. \end{aligned} \quad (3)$$

For a discussion on how a constant velocity profile can be achieved by specifying $\eta(\tau)$ in a different way, the reader is referred to Häusler et al. (2009a). A feasible trajectory can now be obtained by solving

$$\min_{\Xi} J \quad \text{subject to geometric boundary conditions and (3) for all } i \in [1, \ldots, n] \tag{F1}$$

where Ξ is the vector of optimization parameters, that may include τ_f and the accelerations $\bar{x}''(0)$, $\bar{y}''(0)$ and $\bar{z}''(0)$. Also, one could also think of including the jerk $\bar{x}'''(0)$ etc., if (1) is adapted accordingly.

2.2 Cost function considerations.

Imagine a vehicle moving around a circumference: in the simplest case, i.e. with negligible sideslip, constant speed, and without current, the propulsion system only needs to counteract the drag. In case the vehicle is experiencing

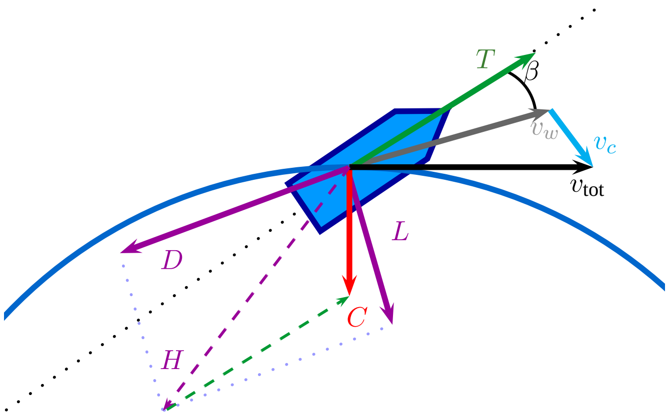

Fig. 2. The forces acting upon a vehicle moving around a circumference with constant speed. Here, v_{tot} is the total velocity and v_w is the velocity with respect to the fluid.

current influence, the situation is as depcited in Fig. 2: the vehicle's speed with respect to the water, v_w has to be oriented in a manner that allows it to counteract the current speed in such a way that the total resulting velocity matches the one required by the computed velocity profile, tangential to the path. The thrust T is always collinear with the vehicle's body axis, but because of the sideslip β, the vehicle's motion with respect to the water differs from the direction of thrust. The drag force D acting on the vehicle is always collinear with its direction of movement; the lift force L is always perpendicular to D. The total hydrodynamic force created by D and L again needs to be compensated by T so as to meet the requirement that the centripetal force is pointing towards the center of the circumference, which defines the magnitude and direction of thrust needed to move the vehicle with a constant speed.

For a thorough treatment of the mechanics of computing each force's influence on the vehicle movement correctly, the reader is referred to e.g. Spong and Vidyasagar (1989). In this paper, we are neglecting the vehicle dynamics and write the cost function J simply as

$$J = \int_0^{t_f} (D + T)\, v_w(t) dt = \int_0^{t_f} \left[\frac{1}{2} \rho C_d v_w^2(t) A + m a_w(t) \right] v_w(t) dt, \tag{4}$$

where ρ is dynamic pressure, C_d is the total drag coefficient of the vehicle, A its reference area and m its mass. The subscript $_w$ denotes the vectors with respect to the fluid.

3. DECONFLICTED MULTIPLE VEHICLE PATHS

The above methodology is now extended to deal with multiple vehicles. In particular, we address the problem of time-coordinated control where all vehicles must arrive at their respective final destinations at the same time. The dimension of the corresponding optimization problem increases and the time coordination requirement introduces additional constraints on the parameters τ_i, where $i = 1, \ldots, n$ is the number of vehicles. To achieve simultaneous time of arrival, we adopt the functions

$$\eta_i(\tau_i) = \eta_i(0) + \frac{\tau_i}{\tau_{f_i}} (\eta_i(\tau_{f_i}) - \eta_i(0)).$$

Other definitions of $\eta(\tau)$ are possible; they be used to meet other planning requirements such as constant speed; see Häusler et al. (2009a). Integrating $\dot{\tau}_i = \eta_i(\tau_i)$ yields

$$\tau_{f_i} = \tau_i(t_f) = \begin{cases} \eta_i(0) t_f & \eta_i(\tau_{f_i}) = \eta_i(0) \\ \dfrac{\eta_i(\tau_{f_i}) - \eta_i(0)}{\ln\left(\frac{\eta_i(\tau_{fi})}{\eta_i(0)}\right)} t_f & \eta_i(\tau_{f_i}) \neq \eta_i(0) \end{cases} \tag{5a}$$

and

$$\frac{t}{t_f} = \begin{cases} \dfrac{\tau_i}{\tau_{f_i}} & \eta_i(\tau_{f_i}) = \eta_i(0) \\ \dfrac{\ln\left(1 + \left(\frac{\eta_i(\tau_{fi})}{\eta_i(0)} - 1\right) \frac{\tau}{\tau_f}\right)}{\ln\left(\frac{\eta_i(\tau_{fi})}{\eta_i(0)}\right)} & \eta_i(\tau_{fi}) \neq \eta_i(0) \end{cases} \tag{5b}$$

Considering t_f, in some specified interval $[t_1, t_2]$, as the key search parameter in an optimization problem, the final values τ_{f_i} of the path parameters τ_i are uniquely defined by (5a). This can now be used to achieve either spatial (paths are separated "geometrically") or temporal deconfliction (paths are allowed to intersect or violate the clearance condition E if the vehicles are not within the conflicting region at the same instance of time). The elegance of using our approach for multiple vehicle path planning lies in the fact that it guarantees *exact* equal times of arrival. Simulation results illustrating the difference between the two types of deconfliction are shown in Figure 3.

All of the graphs presented in this paper show results of the problem of path generation for two vehicles under the assumption that the angle of sideslip β is negligible small. Moreover, the initial headings $\psi_1(0)$ and $\psi_2(0)$ are open for optimization, where the initial guesses are the original vehicle headings ψ_{1_0} and ψ_{2_0}. All other initial guesses are set to 0 with the exception of the guess of the arrival time $t_f =$ 300s. In total, the design variable vector used in all scenarios presented here is the vector $I \in \mathbb{R}^9$ and has the shape $I = \left[t_f \ \psi_1(0) \ \theta_1(0) \ |\ddot{p}_1(0)| \ |\ddot{p}_1(t_f)| \ \psi_2(0) \ \theta_2(0) \ |\ddot{p}_2(0)| \ |\ddot{p}_2(t_f)| \right]^\mathsf{T}$, where $\theta_i(\cdot)$ is the pitch angle and is always 0 in the presented 2D cases. I can easily be shaped according to one's requirements, e.g. to include the initial velocities $\dot{p}_i(0)$ as further design variables.

3.1 Spatial deconfliction.

In the case of spatial deconfliction, feasible trajectories for all the vehicles are obtained by solving an optimization problem of the form

$$\left. \begin{array}{l} \displaystyle\min_{\Xi_i, i=1,\ldots,n} \sum_{i=1}^{n} w_i J_i \quad \text{subject to geometric boundary conditions and (3) for any } i \in [1, \ldots, n], \text{ and} \\ \displaystyle\min_{j,k=1,\ldots,n, j \neq k} ||\bar{p}_{c_j}(\tau_j) - \bar{p}_{c_k}(\tau_k)||^2 \geq E^2 \\ \text{for any } \tau_j, \tau_k \in [0, \tau_{f_j}] \times [0, \tau_{f_k}] \text{ with } \tau_{f_j}, \tau_{f_k} \text{ obtained from (5a) and } t_f \in [t_1, t_2] \end{array} \right\} \tag{F2}$$

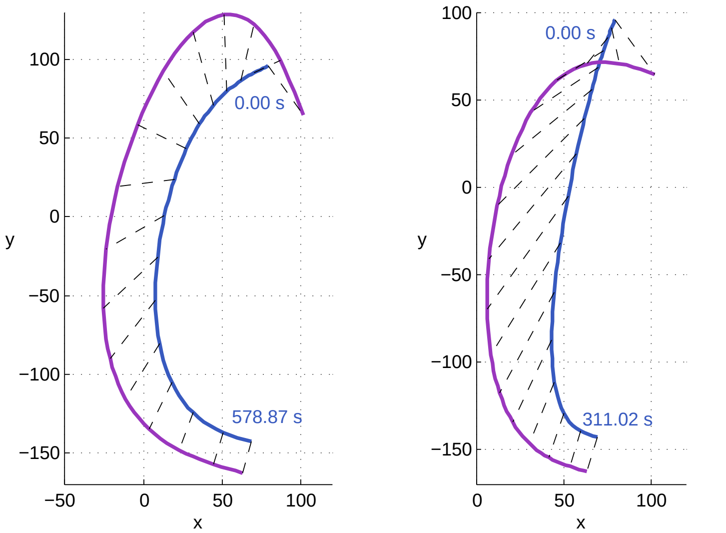

(a) Spatial deconfliction with active communication constraint $C = 50$m.

(b) Temporal deconfliction with $C = 80$m.

	p_1	p_2
$v_{\min}$	$0.2\frac{\text{m}}{\text{s}}$	$0.1\frac{\text{m}}{\text{s}}$
$v_{\max}$	$1.5\frac{\text{m}}{\text{s}}$	$1.3\frac{\text{m}}{\text{s}}$
$[x_0, y_0]$	$[79.22, 95.95]$m	$[101.78, 64.53]$m
$[x_f, y_f]$	$[68.90, -143.05]$m	$[63.27, -162.91]$m
ψ_0	$236.07°$	$244.34°$
ψ_f	$-15.82°$	$-15.82°$
v_0	$0.25\frac{\text{m}}{\text{s}}$	$1.03\frac{\text{m}}{\text{s}}$
v_f	$0.62\frac{\text{m}}{\text{s}}$	$0.62\frac{\text{m}}{\text{s}}$

(c) The randomly generated boundary conditions used throughout this paper.

Fig. 3. Algorithm runs for spatial and temporal deconfliction with clearance $E = 5$m.

where J_i represents total energy consumption of vehicle V_i and the weights $w_i > 0$ penalize the energy consumptions of all vehicles. Note that in contrast to (F1), in (F2) an additional constraint was added to guarantee spatially deconflicted trajectories separated by a minimum spatial clearance distance E.

In summary, we seek to minimize the used energy, given the t_f that is changed during the optimization runs, and subject to constraints that include minimum and maximum vehicle speeds, maximum vehicle accelerations, the allowed window of times of arrival, and spatial clearance requirements for deconfliction.

3.2 Temporal deconfliction.

Temporal deconfliction introduces an extra degree of freedom (time), that is not available in the case of spatial deconfliction. As such, it yields solutions whereby paths are allowed to come to close vicinity or intersect in space. For achieving temporal deconfliction, the key step involves changing the collision avoidance constraint in (F2) to

$$||p_i(t) - p_j(t)||^2 \geq E^2, \quad \forall\, i, j = 1, \ldots, n; i \neq j \text{ and } t \in [0, t_f], \qquad (6)$$

where t_f is the optimization parameter and t is related to the τ_i via (5b). Notice that temporally deconflicted path planning for multiple vehicles is the first step in the general methodology introduced in Ghabcheloo et al. (2009).

4. INCORPORATING ENVIRONMENTAL RESTRICTIONS

The constraints nature poses onto a given mission include, but are by no means limited to, ocean currents and obstacles such as ocean vessels and landmasses. Limitations in communication range are counted to the environmental conditions as well. All of these constraints have been incorporated into the optimization by employing the barrier function method described in Hauser and Saccon (2006). In the remainder of this section, we show results obtained through simulation.

First, let us consider the effect of ocean currents onto the planned paths. Of course, currents can and have to be taken care of the path following controller of the vehicle, and one might ask why to incorporate ocean currents already at the path planning level. This is due to the fact that although the vehicle might be able to track a given path correctly, this path might not be the most energy efficient one for facing a given current, i.e. time-optimal paths depend on currents (see also Kruger et al. (2007)). This can be taken into account by including the effects of external currents when computing the required propulsion energy in (4). The effect of this is shown in Figure 4.

Not only do current effects play a major role in shaping a path, but also the effects imposed on a multiple vehicle constellation through restrictions in communication. Fig. 3(b) shows first results where the communication constraint has been implemented in a way that defines a loss of communication between both vehicles as exceeding the maximum permissible distance C. Although the formulation is at a very early stage and simplified, the results show that communication constraints influence path shapes and are necessary to include already at the path planning stage.

5. ARCHITECTURE OF THE PATH PLANNER

The requirements imposed onto a versatile path planning algorithm are stated in the schematic shown in Fig. 5. In the first stage, we want to have a means of path generation for single vehicles. This has to take as inputs the boundary conditions, that is initial and final poses (i.e. positions and headings) and has to output a path between those, which is, together with an associated speed-profile, passed onto the optimization algorithm. Additional inputs to the single vehicle path planner are given by the initial guess vector I (see Sec. 3); later on, they will be refined through the optimization process and fed back into the path planner to generate new and improved results.

The different vehicles' dynamic constraints are taken into account as constraints imposed to the optimizer. The optimizing stage takes as inputs the previously generated paths as well as the vehicle dynamic constraints (e.g. minimum and maximum permitted velocity magnitudes for each vehicle), constraints imposed by the mission (e.g. spatial clearance and a cost criterion like minimum

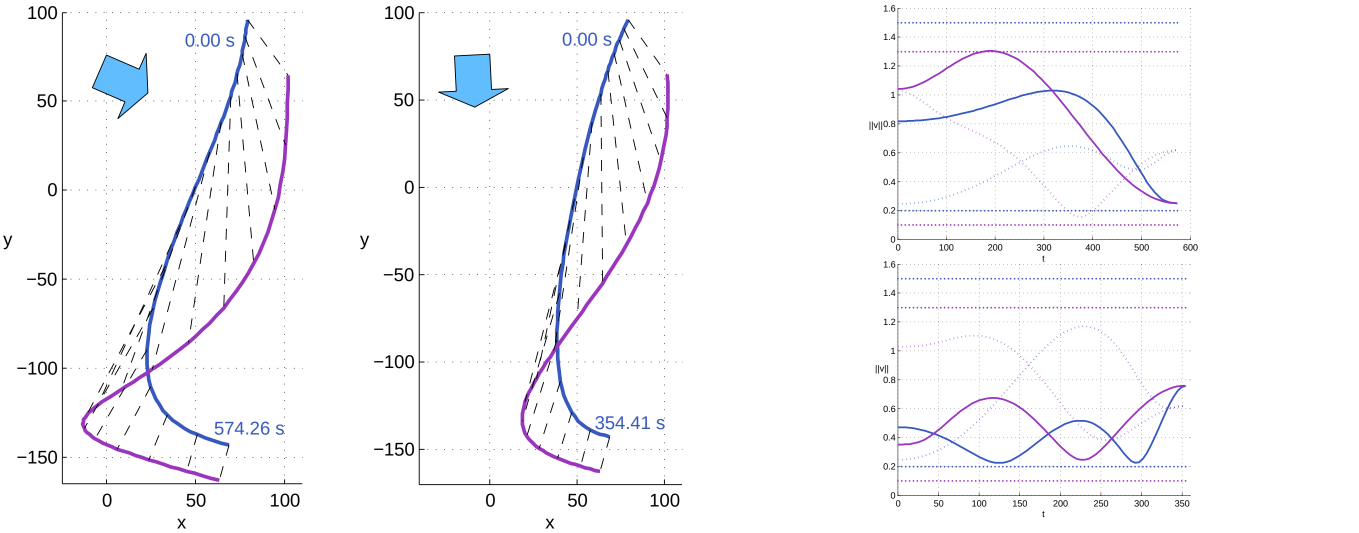

(a) $v_c = 0.85\frac{\text{m}}{\text{s}}$, $\beta_c = 336.24°$. (b) $v_c = 0.68\frac{\text{m}}{\text{s}}$, $\beta_c = 272.79°$. (c) Velocity profiles. The solid lines are $||v_w||$, the dashed lines are $||v_d||$ and the dotted lines are $v_{\min}$ and v_{max}.

Fig. 4. Results of an algorithm run for temporal deconfliction under different current conditions. The planner's result without currents is shown in Figure 3(a) on the right side. The spatial clearance was again $E = 5$m; all other boundary conditions are given in Tab. 3(c).

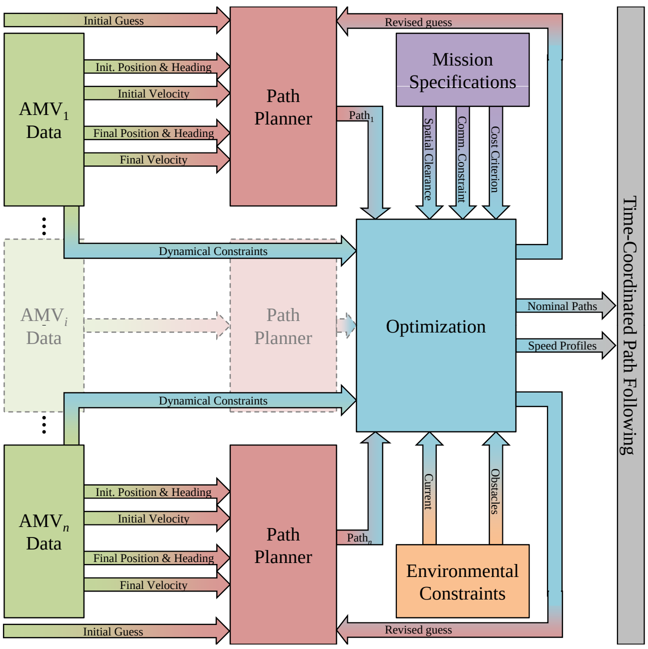

Fig. 5. The multiple vehicle path planning system.

energy usage or minimum simultaneous arrival time), and environmental constraints (such as current speed and direction and obstacles). When the results achieved by repeated calls of the path generator (by the optimization algorithm) cannot be improved any further, the path planning system stops and outputs the paths together with speed profiles, which then can be jointly used in a path following controller.

Algorithmically, this can be expressed as follows:

MultipleVehiclePathPlanner

```
Get boundary conditions B
Get initial guess I
Select mode (spatial/temporal)
Specify constraints (v_min, v_max, a_max, clearance E, etc.)
Choose design variables V for optimization
Define step size vector S and break tolerance T
Ensure SIZE(G) = SIZE(S) = SIZE(V)
Call Init-Hooke-Jeeves(G, S, T)
```

Init-Hooke-Jeeves(G, S, T)

```
for all exploratory and pattern moves of H&J
      do Generate paths with current V from H&J
         Evaluate cost J and weighted constraints C
         if J + C < T
            then break run of H&J
```

6. TIME-COORDINATED PATH FOLLOWING

Given temporally deconflicted paths together with nominal speed profiles generated in the previous sections (or any other methodologies), it now remains to control the vehicles to follow the plan. However, multiple vehicle control schemes that rely on open-loop "pure planning" strategies suffer from following disadvantages. Firstly, should one of the vehicles deviate considerably from its planned trajectory (because of environmental disturbances or temporary failures), replanning becomes necessary. Planning algorithms are in general computationally demanding, and require high communication bandwidth among the vehicles or with a central planning station. Secondly, as it is well known, trajectory tracking suffers from performance limitations that cannot possibly be overcome by any controller structure (see Aguiar et al. (2008)). In this section, we summarize the concept of time-coordinated path following (TC-PF) first introduced in Ghabcheloo et al. (2009). TC-PF is a closed-loop solution to the problem above, and allows us to exploit advantages of path following over trajectory tracking.

Consider a nominal trajectory $p_i(\gamma_i)$ to be followed by vehicle i, parameterized by $\gamma_i \in [0, t_f]$. For the sake of clarity, we refer to the time parameter γ_i as virtual-time. This is done to distinguish it from the real time t that unfolds during the execution of a mission. Further, we let

$\mathsf{p}_i(t)$ denote actual position of AUV i during the mission. We now make the key observation that virtual-time can be simply viewed as a variable that parameterizes the spatial paths derived from the trajectories above. These paths, together with the resulting vehicle speed assignments (specified as functions of γ_i), are all that is required for path following, which will dictate how γ_i actually evolves in time.

Assume each AUV is equipped with a path-following control strategy that keeps the following error

$$e_{\mathsf{p}_i}(t) = ||\mathsf{p}_i(t) - p_i(\gamma_i(t))|| \quad (7)$$

small. The generated trajectories $p_i(\gamma_i)$ guarantee the following two facts: 1) if $\forall t > 0, \gamma_i(t) = \gamma_j(t)$, then vehicle i and vehicle j will remain deconflicted; 2) vehicle i will follow its trajectory as planned if $\gamma_i(t) = t$. In the non ideal case where due to disturbances the vehicles deviate from the planned trajectories, one must guarantee that the vehicles will remain deconflicted. Therefore, we would like to derive time coordination control laws for $\dot{\gamma}_i(t)$ in such a way that

$$e_{c_i}(t) = \|\gamma_j(t) - \gamma_i(t)\| < \delta, \quad (8)$$

for some $\delta > 0$, and in the absence of disturbances, the dynamics of $\dot{\gamma}_i$ must verify $\dot{\gamma}_i(t) = 1$, so as to recover the planned trajectories and optimality is retained. Notice that the mission will be "near optimal" in the presence of disturbances. The rationale behind the bounds on the errors will become clear next: using the mean value theorem, it is easily shown that

$$\|p_i(t_a) - p_i(t_b)\| < v_{max}|t_a - t_b|; \forall i, \quad (9)$$

and that the trajectories are deconflicted in time to satisfy

$$\|p_i(t_a) - p_j(t_a)\| > E; \quad \forall t_a \in [0, t_f], \quad (10)$$

for all $i, j;\ i \neq j$. Comparing equations (7)-(10), if we neglect path-following error, it can be shown that, as mision unfolds, clearances remain bounded and satisfy the following inequality

$$\|\mathsf{p}_i(t) - \mathsf{p}_j(t)\| > \bar{E} \quad (11)$$

where $\bar{E} = E - \delta v_{max}$. Notice that $\bar{E} < E$, thus during planning phase, we must take into account higher clearance values.

To meet the objectives above, for each vehicle the nominal speed profile is perturbed by a corrective speed $\tilde{v}_i$, that is function of the errors $|\gamma_i - \gamma_j|$ so as to keep the latter small and to drive them to zero in the absence of disturbances. These adjustments are done by exchanging coordination information (virtual-time variables γ_i) among vehicles using the supporting communication network. In practice, some assumptions must me made with respect to the connectivity of the underlying communication graph to ensure adequate behaviour of the coordination system. Another issue of considerable importance is the impact of the rate of communications on the convergence rates of appropriately defined error variables. The less communication losses, the faster convergence is. Thus, we incorporated the communication requirements to decrease probabilities of communication losses. (See Ghabcheloo et al. (2009) for more details on TC-PF.)

7. CONCLUSION

In this paper we showed the most recent improvements of our path planning algorithm for multiple marine vehicles. Although it proves increasing versatility, there remains a number of problems that still have to be tackled. In a recent internal report we were able to show that the runtime increases exponentially in terms of the number of computed discrete path points, which suggests to use a different kind of optimization approach (see e.g. Hauser (2002); Hauser and Saccon (2006)) and/or a different means of mathematical path description. Additionally, the communication constraint currently is simply a path distance formulation with respect to traversal time, i.e. the paths are not allowed to be further apart than a given distance at any instance of time. This can be improved in various ways; for example, a penalty could be put on the number of communication losses, so that short interruptions would be allowed. Last, but not least, the energy computation has to be argued about more carefully (see e.g. Harvald (1983)), and the vehicle dynamics have to be incorporated so as to accurately match the actual energy consumption, especially in the case of non-constant vehicle velocity.

ACKNOWLEDGEMENTS

The authors would like to thank *Prof. John Hauser* from the University of Boulder in Colorado for his much appreciated comments and help in fixing some notational issues. We also want to thank *Luís Sebastião* for his hints on the energy calculation in Section 2.

REFERENCES

FREE$_{\text{sub}}$*NET* (2006–2010). A Marie Curie Research Training Network. URL `http://www.freesubnet.eu`.

Aguiar, A.P., Hespanha, J.P., and Kokotovic, P. (2008). Performance Limitations in Reference-Tracking and Path-Following for Nonlinear Systems. In *IFAC Automatica*, volume 44, 598–610. San Francisco (CA), USA.

Ghabcheloo, R., Kaminer, I., Aguiar, A.P., and Pascoal, A. (2009). A General Framework for Multiple Vehicle Time-Coordinated Path Following Control. *Proceedings of the American Control Conference (ACC 2009)*.

GREX (2006–2009). Coordination and Control of Cooperating Heterogeneous Unmanned Systems in Uncertain Environments. URL `http://www.grex-project.eu`.

Harvald, S.A. (1983). *Resistance and Propulsion of Ships*. John Wiley and Sons, USA.

Hauser, J. (2002). A Projection Operator Approach to the Optimization of Trajectory Functionals. In *IFAC World Congress*.

Hauser, J. and Saccon, A. (2006). A Barrier Function Method for the Optimization of Trajectory Functionals with Constraints. In *45th IEEE Conference on Decision and Control*, 864–869.

Häusler, A.J., Ghabcheloo, R., Kaminer, I., Pascoal, A.M., and Aguiar, A.P. (2009a). Path Planning for Multiple Marine Vehicles. In *Proceedings of the IEEE Oceans '09*. Bremen, Germany.

Häusler, A.J., Ghabcheloo, R., Pascoal, A.M., Aguiar, A.P., Kaminer, I.I., and Dobrokhodov, V.N. (2009b). Temporally and Spatially Deconflicted Path Planning for Multiple Autonomous Marine Vehicles. In *Proceedings of the* 8^{th} *Conference on Manoeuvring and Control of Marine Craft*. Guarujá (SP), Brazil.

Hooke, R. and Jeeves, T. (1961). A "Direct Search" Solution of Numerical and Statistical Problems. *Journal of ACM*, 212–229.

Kaminer, I., Yakimenko, O.A., Dobrokhodov, V., Pascoal, A., Hovakimyan, N., Cao, C., Young, A., and Patel, V. (2007). Coordinated Path Following for Time-Critical Missions of Multiple UAVs via $\mathcal{L}_1$ Adaptive Output Feedback Controllers. *AIAA Guidance, Navigation and Control Conference and Exhibit*.

Kaminer, I., Yakimenko, O.A., Pascoal, A., and Ghabcheloo, R. (2006). Path Generation, Path Following and Coordinated Control for Time-Critical Missions of Multiple UAVs. *Proceedings of the 2006 American Control Conference*.

Kruger, D., Stolkin, R., Blum, A., and Briganti, J. (2007). Optimal AUV Path Planning for Extended Missions in Complex, Fast-Flowing Estuarine Environments. In *2007 IEEE International Conference on Robotics and Automation*, 4265–4270.

Spong, M.W. and Vidyasagar, M. (1989). *Robot Dynamics and Control*. John Wiley & Sons.

Yakimenko, O. (2000). Direct Method for Rapid Prototyping of Near-Optimal Aircraft Trajectories. In *AIAA Journal of Guidance, Control and Dynamics*, volume 23, 865–875.